Kaonic nuclei studied based on a new framework of antisymmetrized molecular dynamics

Akinobu Doté,[1] Hisashi Horiuchi,[2] Yoshinori Akaishi,[1,3] and Toshimitsu Yamazaki[4]
[1]*Institute of Particle and Nuclear Studies, KEK, Tsukuba, Ibaraki 305-0801, Japan*
[2]*Department of Physics, Kyoto University, Kyoto 606-8502, Japan*
[3]*College of Science and Technology, Nihon University, Funabashi 274-8501, Japan*
[4]*RI Beam Science Laboratory, RIKEN, Wako, Saitama 351-0198, Japan*
(Received 9 March 2004; published 20 October 2004)

We have developed a new framework of antisymmetrized molecular dynamics (AMD), to adequately treat the $I=0$ $\bar{K}N$ interaction, which is essential to study kaonic nuclei. The improved points are 1) $pK^-/n\bar{K}^0$ mixing and 2) total spin and isospin projections. These improvements enable us to investigate various kaonic nuclei ($ppnK^-$, $pppK^-$, $pppnK^-$, ^{6}BeK^-, ^{9}BK^-, and ^{11}CK^-) systematically. We have found that they are deeply bound and extremely dense with a variety of shapes.

DOI: 10.1103/PhysRevC.70.044313 PACS number(s): 21.80.+a, 13.75.Jz, 21.30.Fe, 21.45.+v

I. INTRODUCTION

Recently, it has been shown theoretically that a K^- meson can be deeply bound in light nuclei as a discrete state, such as ^{3}He$+K^-$, ^{4}He$+K^-$, and ^{8}Be$+K^-$, where the K^- meson makes the nucleus shrink drastically to form a dense state [1]. Exotic proton-rich bound systems with $\bar{K}$, ppK^-, $pppK^-$, $pppnK^-$, and ^{9}B$+K^-$, are expected to be produced in (K^-,π^-) reactions [2]. In our previous paper, we investigated kaonic nuclei, which are denoted as $\bar{K}$ nuclei hereafter, ^{3}He $+K^-$ and ^{8}Be$+K^-$, with a simple version of antisymmetrized molecular dynamics (AMD) [3,4]. Although our results are similar to those obtained in Ref. [1], a strange property appeared in ^{8}Be$+K^-$. It is an isovector deformation, which means that the proton distribution differs from the neutron one in spite of $N=Z$. Thus, $\bar{K}$ nuclei seem to provide interesting phenomena and stimulate further studies.

Apparently, these interesting properties of $\bar{K}$ nuclei can be attributed to the bare $\bar{K}N$ interaction. In particular, the $I=0$ $\bar{K}N$ interaction plays an essential role. According to a precise experiment [5], the 1*s* atomic state of a kaonic hydrogen (i.e., proton$+K^-$) is shown to be shifted upward. This upward shift, which is consistent with the low-energy scattering data of $\bar{K}N$ [6], suggests that the $\bar{K}N$ interaction is strongly attractive, so that the system of a K^- and a proton has a nuclear bound state which corresponds to the $I=0$ $\Lambda(1405)$ hyperon resonance lying at 27 MeV below the K^-p threshold. In a boson exchange potential model, the Jülich group [7] showed that all of the ω, ρ, and σ mesons work coherently to give a strong attraction between a $\bar{K}$ and an N which accommodates a K^--p bound state, identified as $\Lambda(1405)$. Studies based on chiral SU(3) [8] also show that the $I=0$ $\bar{K}N$ interaction is attractive enough to form a $\Lambda(1405)$. The phenomenological $\bar{K}N$ interaction [1], which we employ as a *bare* $\bar{K}N$ interaction, is similar to those led by the chiral SU(3) and boson exchange theories. Since the $I=0$ $\bar{K}N$ interaction is much more attractive than the $I=1$ one, a K^- meson attracts protons rather than neutrons, causing an isovector deformation. Thus, the $I=0$ $\bar{K}N$ interaction is essential for studying $\bar{K}$ nuclei.

In this paper we present systematic studies of $\bar{K}$ nuclei with AMD. Since AMD treats a system in a fully microscopic way without any assumption concerning the structure of the system, it is suitable for studying $\bar{K}$ nuclei, whose structures might be exotic. The simple version of AMD [3], however, has a technical problem in treating the $I=0$ $\bar{K}N$ interaction, which dominates $\bar{K}$ nuclear systems: it cannot include the degree of freedom of $\bar{K}^0$, and fails to describe the $I=0$ $\bar{K}N$ state. Therefore, in our previous paper we dealt with the $I=0$ $\bar{K}N$ interaction by incorporating its $\bar{K}^0n$ part effectively into the K^-p interaction. Of course, the $I=0$ $\bar{K}N$ interaction should be treated as precisely as possible, because it plays an essential role in $\bar{K}$ nuclei. In this paper, we improve the framework of AMD so that it can treat the $I=0$ $\bar{K}N$ interaction adequately. We introduce the degree of freedom of $\bar{K}^0$ into the model space of AMD ("$pK^-/n\bar{K}^0$ mixing"). Since $\bar{K}$ nuclear states depend largely on their isospin due to the strong isospin-dependence of the $\bar{K}N$ interaction, we carry out the isospin projection as well as the angular momentum projection ("J and T projections") of the obtained intrinsic state. With the new version of AMD, we systematically investigate a variety of $\bar{K}$ nuclei. We try to answer the following questions: (i) What $\bar{K}$ nuclei are deeply bound with narrow widths? (ii) Is there any strange structure peculiar to $\bar{K}$ nuclei?

This paper is composed as follows: In Sec. II, we present the improvements of AMD; $pK^-/n\bar{K}^0$ mixing, J and T projections, and other formalisms. In Sec. III, we demonstrate the capability of our new framework, and then apply it to various $\bar{K}$ nuclei ($ppnK^-$, $pppK^-$, $pppnK^-$, ^{6}BeK^-, ^{9}BK^-, and ^{11}CK^-). The results and discussion are given in Sec. IV. We summarize our study in Sec. V.

II. FORMALISM

In the present study, we employ the AMD approach as a means of studying $\bar{K}$ nuclei. It has succeeded in studying the structures of light unstable nuclei [9]. In particular, it is powerful for investigating the global properties of many light nuclei systematically. We know that various few-body methods, such as summarized in Ref. [10], can treat few-body $\bar{K}$ nuclei more accurately than AMD. Compared with these usual methods, AMD is more handy and applicable to more complex nuclei. Our aim is a systematic study of a variety of $\bar{K}$ nuclei.

In the simple version of AMD employed in our previous study, we restricted its model space to the proton, neutron and K^- meson. Due to the lack of $\bar{K}^0$ in the model space, we could not describe the $I=0$ $\bar{K}N$ state,

$$|\bar{K}N(I=0)\rangle = \frac{1}{\sqrt{2}}(|pK^-\rangle + |n\bar{K}^0\rangle). \tag{1}$$

In other words, we could not precisely treat the coupling of the pK^- pair with the $n\bar{K}^0$ one through the $I=0$ $\bar{K}N$ interaction in the particle basis treatment of AMD. In the previous study, we incorporated all contributions from the $I=0$ $\bar{K}N$ interaction into an effective K^-p interaction, as follows:

$$V_{K^-p} = \alpha V_{\bar{K}N(I=0)} + \beta V_{\bar{K}N(I=1)}, \tag{2}$$

where α and β are some constants determined by counting the number of $I=0$ pairs and $I=1$ ones in a given state of total isospin T. For example, we set $(\alpha,\beta)=(\frac{3}{4},\frac{1}{4})$ in the case of $ppnK^-$ $(T=0)$. However, we have to check how this prescription is reliable for various $\bar{K}$ nucleus cases. For this purpose, we introduce the degree of freedom of $\bar{K}^0$ into the AMD framework to treat " $pK^-/n\bar{K}^0$ mixing" directly.

A. $pK^-/n\bar{K}^0$ mixing

First, we explain our idea for the simple case of a $\bar{K}$ nucleus $ppnK^-$. In this $\bar{K}$ nucleus, the component of $pnn\bar{K}^0$ is mixed because a pair of pK^- is replaced with that of $n\bar{K}^0$ by the $I=0$ $\bar{K}N$ interaction. Hereafter, we express this state as ${}^3_{\bar{K}}$H. An ordinary way to treat it is to perform a coupled channel calculation, preparing several Slater determinants for both channels of $ppnK^-$ and $pnn\bar{K}^0$. In the present paper, we deal with such systems where several channels are coupled as follows: In stead of multi Slater determinants, we employ a single Slater determinant with *charge-mixed* single particle wave functions, i.e.,

$$|N_i\rangle = x_i|p\rangle + y_i|n\rangle, \tag{3}$$

$$|K\rangle = z|K^-\rangle + w|\bar{K}^0\rangle, \tag{4}$$

where $|N_i\rangle$ and $|K\rangle$ indicate a single nucleon wave function and a $\bar{K}$ meson wave function, respectively. $|N_i\rangle$ can describe the state where a proton and a neutron are mixed, and also $|K\rangle$ can describe the state where K^- and $\bar{K}^0$ are mixed. With these wave functions we describe ${}^3_{\bar{K}}$H as $|\det[N_1N_2N_3]K\rangle$. This state contains the component of $|pnn\bar{K}^0\rangle$ as well as that of $|ppnK^-\rangle$. In this method, since each nucleon has a chance to be a proton or a neutron, the important channel is automatically chosen in the process of the energy variation. In addition, we expect that $|\det[N_1N_2N_3]K\rangle$ can represent a state in which the contribution of several configurations is coherently additive: for example, if two configurations such as $|ppnK^-\rangle$ and $|pnn\bar{K}^0\rangle$ work coherently, such state is represented as $|p(p+n)n(K^-+\bar{K}^0)\rangle$.

However, we remark one point: $|\det[N_1N_2N_3]K\rangle$ is likely to have incorrect components, for example $pppK^-$, $ppn\bar{K}^0$, etc. which should not couple with ${}^3_{\bar{K}}$H. To avoid the mixing of such incorrect components, we project it onto a state whose isospin-z component T_z is equal to that of ${}^3_{\bar{K}}$H.

Now, we show the details of our wave function based on the concept of $pK^-/n\bar{K}^0$ mixing. Our nucleon wave function, $|\varphi_i\rangle$, is represented by the superposition of several Gaussian wave packets [11],

$$|\varphi_i\rangle = \sum_{\alpha=1}^{N_n} C_\alpha^i \exp\left[-\nu\left(\boldsymbol{r} - \frac{\boldsymbol{Z}_\alpha^i}{\sqrt{\nu}}\right)^2\right]|\sigma_i\rangle|\tau_\alpha^i\rangle. \tag{5}$$

Namely, the ith nucleon is described by the superposition of N_n Gaussian wave packets whose centers are $\{\boldsymbol{Z}_\alpha^i\}$. $|\sigma_i\rangle$ means a spin wave function, and is $|\uparrow\rangle$ or $|\downarrow\rangle$. $|\tau_\alpha^i\rangle$ means an isospin wave function, and has the following form:

$$|\tau_\alpha^i\rangle = \left(\frac{1}{2} + \gamma_\alpha^i\right)|p\rangle + \left(\frac{1}{2} - \gamma_\alpha^i\right)|n\rangle, \tag{6}$$

where γ_α^i is a variational parameter. In the usual AMD the isospin of each nucleon does not change, i.e., in the process of energy variation the protons remain as protons and the neutrons as neutrons. However, in the present paper we make the isospins of all nucleons changeable so that we can treat $pK^-/n\bar{K}^0$ mixing. In the same way, a $\bar{K}$ meson wave function, $|\varphi_K\rangle$, has the form

$$|\varphi_K\rangle = \sum_{\alpha=1}^{N_K} C_\alpha^K \exp\left[-\nu\left(\boldsymbol{r} - \frac{\boldsymbol{Z}_\alpha^K}{\sqrt{\nu}}\right)^2\right]|\tau_\alpha^K\rangle. \tag{7}$$

Here, the isospin wave function of a $\bar{K}$, $|\tau_\alpha^K\rangle$, as well as that of a nucleon, is changeable,

$$|\tau_\alpha^K\rangle = \left(\frac{1}{2} + \gamma_\alpha^K\right)|\bar{K}^0\rangle + \left(\frac{1}{2} - \gamma_\alpha^K\right)|K^-\rangle. \tag{8}$$

Because a nucleon is a Fermion, we antisymmetrize the wave function of the nucleon's system, $|\Phi_N\rangle=\det[|\varphi_i(j)\rangle]$. Then, the $\bar{K}$ meson wave function is combined to it, $|\Phi\rangle = |\Phi_N\rangle\otimes|\varphi_K\rangle$. Moreover, we project the total wave function onto the eigenstate of parity,

$$|\Phi^\pm\rangle = \frac{1}{\sqrt{2}}[|\Phi\rangle \pm \mathcal{P}|\Phi\rangle]. \tag{9}$$

If we perform an energy variation with a trial wave function Eq. (9), it is likely that the z component of the isospin (T_z) of the total system is different from that of a $\bar{K}$ nucleus that we try to calculate originally. To avoid any mixing of components having an incorrect T_z, we project the total system onto an eigenstate of T_z before the energy variation,

$$|\hat{P}_M\Phi^{\pm}\rangle = \int d\theta \exp[-i\theta(\hat{T}_z - M)]|\Phi^{\pm}\rangle. \tag{10}$$

Thus, we can obtain a wave function containing only the components of $T_z=M$. We utilize $|\hat{P}_M\Phi^{\pm}\rangle$ as a trial wave function.

Our wave function includes complex number parameters $\{X^i_\alpha\}\equiv\{C^i_\alpha, \boldsymbol{Z}^i_\alpha, \gamma^j_\alpha; C^K_\alpha, \boldsymbol{Z}^K_\alpha\ \gamma^K_\alpha\}$ and a real number parameter (ν). These are determined by the frictional cooling equation, as mentioned in Sec. II D.

In the present study, we use a common width parameter (ν) of a Gaussian wave packet for a nucleon and for a $\bar{K}$ meson so as to simplify our calculation. However, it seems natural that the spreading width of a nucleon is different from that of a $\bar{K}$ meson. We take this point into account by using different numbers of Gaussian wave packets for a nucleon and a $\bar{K}$ meson, i.e., N_n in Eq. (5) is not equal to N_K in Eq. (7).

B. *J* and *T* projections

The angular momentum projection (J projection) is necessary to study $\bar{K}$ nuclei as well as usual nuclei. In addition, the isospin projection (T projection) also seems to be important because the $\bar{K}N$ interaction has strong isospin dependence. Therefore, we perform angular-momentum and isospin projections simultaneously. J projection is done numerically by rotating the system in space, as has often been done. T projection is performed in quite the same way, but by rotating in isospin space. Our J and T projections are as follows:

$$|\hat{P}^J_{MK}\,\hat{P}^T_{T_zT'_z}\Phi^{\pm}\rangle = \int d\Omega_{\text{ang.}} D^{J*}_{MK}(\Omega_{\text{ang.}})\hat{R}_{\text{ang.}}(\Omega_{\text{ang.}}) \times \int d\Omega_{\text{iso.}} D^{T*}_{T_zT'_z}(\Omega_{\text{iso.}})\hat{R}_{\text{iso.}}(\Omega_{\text{iso.}})|\Phi^{\pm}\rangle, \tag{11}$$

where $|\Phi^{\pm}\rangle$ is the intrinsic wave function, which is already determined by the frictional cooling equation, as shown in Sec. II D. We calculate various expectation values with $|\hat{P}^J_{MK}\,\hat{P}^T_{T_zT'_z}\Phi^{\pm}\rangle$.

C. Hamiltonian

Our Hamiltonian in AMD calculations,

$$\hat{H} = \hat{T} + \hat{V}_{NN} + \hat{V}_C + \hat{V}_{KN} - \hat{T}_G, \tag{12}$$

is composed of the kinetic energy $\hat{T}$, the effective NN potential $\hat{V}_{NN}$, the Coulomb force $\hat{V}_C$, and the effective $\bar{K}N$ potential $\hat{V}_{KN}$. The center-of-mass motion energy, $\hat{T}_G$, is subtracted. In the kinetic energy and the center-of-mass motion energy, we treat the mass difference between a nucleon and a $\bar{K}$ meson correctly. For example, the kinetic energy is

$$\hat{T} = \sum_{i=1}^{A} \frac{\hat{\boldsymbol{p}}_i^2}{2m_N} + \frac{\hat{\boldsymbol{p}}_K^2}{2m_K}, \tag{13}$$

where m_N and m_K indicate the mass of a nucleon and that of K^-, respectively. The Coulomb force is represented by the superposition of seven-range Gaussians [12].

In the study of $\bar{K}$ nuclei, we do not use existing effective interactions which may be justified for studying phenomena around the normal density. Since the system is likely to become extremely dense due to the strong $\bar{K}$ attraction, we employ the g-matrix method [1]. We adopt the Tamagaki potential (OPEG) [13] as a bare NN interaction, and the Akaishi-Yamazaki $\bar{K}N$ potential [1] as a bare $\bar{K}N$ interaction. Because the Tamagaki potential can reproduce NN phase shifts up to 660 MeV in the laboratory system [13], we expect that it can be applied to such extremely dense states. The effective $NN/\bar{K}N$ interactions constructed from the bare ones are represented by the following ten-range Gaussians:

$$V^X_{NN}(r) = \sum_{a=1}^{10} V^X_{NN,a} \exp[-(r/r_a)^2], \tag{14}$$

$$V^I_{\bar{K}N}(r) = \sum_{a=1}^{10} V^I_{\bar{K}N,a} \exp[-(r/r_a)^2], \tag{15}$$

"X" in Eq. (14) is ${}^1E, {}^3E, {}^1O$, or ${}^3O$, and "I" in Eq. (15) is 0 or 1. We use these $V^X_{NN}(r)$ and $V^I_{\bar{K}N}(r)$ as effective $NN/\bar{K}N$ interactions in our AMD calculation.

Our procedure is as follows: (1) For a given density and starting energy of K^-, we construct a g matrix; (2) using the g matrix we carry out the AMD calculation; (3) after the AMD calculation, we check whether or not the obtained density and binding energy of K^- are consistent with those of the g matrix used in the calculation; (4) if no consistency is accomplished, we guess and impose a new density and a new starting energy of K^- for the g matrix calculation by referring to the results obtained so far and return to (1). We repeat this cycle until obtaining a consistent result.

D. Frictional cooling equation with constraint

Our wave function contains complex variational parameters, $\{X^i_\alpha\}=\{C^i_\alpha, \boldsymbol{Z}^i_\alpha, \gamma^j_\alpha; C^K_\alpha, \boldsymbol{Z}^K_\alpha,\ \gamma^K_\alpha\}$. They are determined by the energy variation. In our study, we employ the frictional cooling method as a means of energy variation,

$$\dot{X}^i_\alpha = (\lambda + i\mu)\frac{1}{i\hbar}\left[\frac{\partial\mathcal{H}}{\partial X^{i*}_\alpha} + \eta\frac{\partial\mathcal{W}}{\partial X^{i*}_\alpha}\right] \text{ and c.c.} \tag{16}$$

Here, $\mathcal{H}$ is the expectation value of the Hamiltonian and $\mathcal{W}$ is a constraint condition. η is a Lagrange multiplier, which is determined by $d\mathcal{W}/dt=0$. It is easily proved that, if we as-

TABLE I. Results of $ppnK^-$ in various N_n and N_K. $E(\overline{K})$: binding energy measured from the threshold of $ppn+K^-$. $\rho(0)$: central density. $R_{\rm rms}$, $R^p_{\rm rms}$, $R^n_{\rm rms}$: root-mean-square radii of matter, proton, and neutron, respectively. (β,γ): deformation parameters.

N_n	N_K	$E(\overline{K})$ (MeV)	$\rho(0)$ (fm^{-3})	$R_{\rm rms}$ (fm)	$R^p_{\rm rms}$ (fm)	$R^n_{\rm rms}$ (fm)	β	γ (deg.)
2	5	105.2	1.39	0.72	0.70	0.75	0.19	0.0
3	5	106.3	1.40	0.73	0.70	0.77	0.14	49.0
4	5	109.5	1.41	0.72	0.69	0.78	0.02	49.4
2	8	106.0	1.37	0.72	0.71	0.75	0.19	0.0
2	10	106.2	1.37	0.72	0.71	0.75	0.18	0.0
3	10	107.6	1.41	0.72	0.70	0.77	0.14	51.7
4	10	109.4	1.49	0.71	0.68	0.77	0.00	54.4

sume $\mu<0$ in Eq. (16) and all of the parameters are developed with time according to Eq. (16), the energy of the system decreases while satisfying the constraint condition $\mathcal{W}=0$. If we use the superposition of several Gaussian wave packets to represent a nucleon and a $\overline{K}$ meson wave function, we need a constraint condition in order to fix the center of mass of the total system to the origin, and then W is expressed as follows:

$$\mathcal{W}=\langle\hat{\boldsymbol{R}}_G\rangle^2+\langle\hat{\boldsymbol{P}}_G\rangle^2, \tag{17}$$

$$\hat{\boldsymbol{R}}_G=\frac{\sum_{i=1}^{A} m_N\hat{\boldsymbol{r}}_i+m_K\hat{\boldsymbol{r}}_K}{Am_N+m_K}, \tag{18}$$

$$\hat{\boldsymbol{P}}_G=\sum_{i=1}^{A}\hat{\boldsymbol{p}}_i+\hat{\boldsymbol{p}}_K. \tag{19}$$

III. TESTS OF OUR METHOD

Before applying our method to studies of various $\overline{K}$ nuclei, we investigate the basic properties of our method.

A. Dependence on the number of wave packets

As shown in Eqs. (5) and (7), we represent a single nucleon wave function and a $\overline{K}$ meson wave function with N_n and N_K Gaussian wave packets, respectively. We investigate how much the solution depends on N_n and N_K. First, we perform a test in the case of $ppnK^-$ without $pK^-/n\overline{K^0}$ mixing for simplicity. Table I shows the results of $ppnK^-$ for various N_n and N_K. From this table, we find that the total binding energy and the central density are almost converged up to $N_n=4$ and $N_K=10$. However, we notice that the shape of the system, represented by the deformation parameters (β,γ), is strongly dependent of N_n. This phenomenon can be understood as follows. As mentioned in our previous study [3], the protons distribute compactly near a K^- so as to decrease their total energy by the strongly attractive K^-p interaction. On the other hand, the neutron is widely spread and its total energy decreases by reducing its kinetic energy. Therefore, the protons stay compactly inside the system, while the neutron remains widely outside of the system. Thus, the neutron contributes to the shape of the total system. In the case of $N_n=2$, since the neutron is represented by two Gaussian wave packets, it can spread only linearly. Thus, the total system deforms prolately. In the case of $N_n=3$, it can spread with a triangular shape. Thus, the total system deforms oblately. In the case of $N_n=4$, it can spread with a tetrahedron shape. The total system is therefore spherical. Thus, the shape of the total system changes as N_n is varied.

TABLE II. Quantum numbers before and after projection. J^2_T: $\langle\hat{\boldsymbol{J}}^2\rangle$ of total system. J^2_N, L^2_N, and S^2_N: $\langle\hat{\boldsymbol{J}}^2\rangle$, $\langle\hat{\boldsymbol{L}}^2\rangle$, and $\langle\hat{\boldsymbol{S}}^2\rangle$ of nucleon system. L^2_K: $\langle\hat{\boldsymbol{L}}^2\rangle$ of a $\overline{K}$ meson. T^2 and T_z: $\langle\hat{\boldsymbol{T}}^2\rangle$ and $\langle\hat{T}^z_2\rangle$ of total system.

	J^2_T	J^2_N	L^2_N	S^2_N	L^2_K	T^2	T_z
After	0.75	0.78	0.03	0.75	0.03	0.00	0.00
Before	1.36	1.22	0.44	0.78	0.14	0.02	0.00

Such a dependence of the shape on N_n seems to be peculiar to $ppnK^-$ where the neutron number is equal to 1 and the proton number is 2. In addition, the binding energy measured from the threshold of $ppn+K^-$, $E(\overline{K})$, and the central density do not so strongly depend on N_n and N_K. Therefore, taking the cost-performance of calculations into account, we adopt the model space of $N_n=2$ and $N_K=5$ in our calculations.

B. Solution of $ppnK^-$

We now check whether our new framework, $pK^-/n\overline{K^0}$ mixing and J and T projections, works correctly or not. We perform a test on a system of $ppnK^-$.

First, we investigate the property of J and T projections. Although only the J projection has often been carried out in the study of light unstable nuclei [9,11], the present study for the first time makes the T projection. In Table II, we show various quantum numbers of the wave function before projection ($|\hat{P}_M\Phi^{\pm}\rangle$) and that after projection ($|\hat{P}^J_{MK}\,\hat{P}^T_{T_zT'_z}\Phi^{\pm}\rangle$). Apparently, the ground state of $ppnK^-$ seems to have quantum numbers of $J^\pi=\frac{1}{2}^+$ and $T=0$. We performed J and T projections so that the total system had such quantum numbers. Table II shows that $\langle\hat{\boldsymbol{J}}^2\rangle=0.75$ and $\langle\hat{\boldsymbol{T}}^2\rangle=0.00$, which agree with $J(J+1)=\frac{1}{2}\cdot\frac{3}{2}$ and $T(T+1)=0\cdot1$, respectively. Therefore, it is found that our J and T projections work well.

Next, in Table III various quantities obtained in the present calculation (present) are compared with our previous result of a simple version of AMD (simple AMD) [3] and the result of a BHF calculation (BHF) [1]. This table shows that the present result is almost identical to others. Since the isospin-z component of each particle is changeable in the present framework, we investigated each particle number. Although we calculated $ppnK^-$, the numbers of protons and neutrons after the calculation are both equal to 1.5, while those of K^- and $\overline{K^0}$ are both 0.5. This means that $ppnK^-$ and

TABLE III. Results of $ppnK^-$; $E(\bar{K})$: binding energy measured from the threshold of $ppn+K^-$; Γ: width decaying to $\Lambda\pi$; $\rho(0)$: central density; $R_{\rm rms}$: root-mean-square radius of nucleon system.

	$E(\bar{K})$ (MeV)	Γ (MeV)	$\rho(0)$ (fm^{-3})	$R_{\rm rms}$ (fm)
Present	110.3	21.2	1.50	0.72
Simple AMD	105.2	23.7	1.39	0.72
BHF	108	20	—	0.97

$ppn\bar{K}^0$ are mixed with a ratio of 1:1 as the result of $pK^-/n\bar{K}^0$ coupling through the $I=0$ $\bar{K}N$ interaction.

Here, we remark on the components of the $\bar{K}N$ interaction. We can separate it into three parts in the particle base: (i) V_{nK^-} and $V_{p\bar{K}^0}$, (ii) V_{pK^-} and $V_{n\bar{K}^0}$, and (iii) $V_{pK^-,n\bar{K}^0}$. The interactions (i) and (ii) are working in each channel of $ppnK^-$ and $pnn\bar{K}^0$, and their expectation values are equal to −45 and −255 MeV, respectively. Interaction (iii) is related to $pK^-/n\bar{K}^0$ mixing through the $I=0$ $\bar{K}N$ interaction, and its expectation value is equal to −88 MeV. Thus, we find that the binding of this system is mainly due to the type (ii) interaction and is further supported by the type (iii) interaction, which causes coupling between the two channels.

C. Effect of repulsive core of a bare *NN* interaction

The repulsive core of *NN* interaction plays an essential role in the nuclear shrinkage caused by a K^- meson and the deep binding of a K^- meson. Since the Tamagaki potential (OPEG) can reproduce the *NN* phase shift up to 660 MeV, we expect that it can be applied to very dense system. However, the repulsive core part of the OPEG is represented by a Gaussian form, not by hard core. One may question whether or not a stronger repulsive core still allows the nuclear shrinkage and the deep binding of $\bar{K}$.

Hence, we have investigated the effect of the repulsive core of the *NN* interaction as follows. Since it is often said that the repulsive core lies in the $r<0.4$ fm region of the *NN* interaction, we have regarded such a region of the OPEG as the repulsive core. We have made the potential in the core region more repulsive by multiplying factors of 1.5, 2, and 3. Using such core-enhanced potentials, we have calculated $ppnK^-$ in the same procedure with a simple version of AMD. The total binding energy is obtained to be 109.2, 107.0, and 106.9 MeV for 1.5, 2, and 3 times enhanced core, respectively. It is found that the effect of such core enhancement is saturated at the 2 times case. Thus, $ppnK^-$ is still bound below the $\Sigma\pi$ threshold (106 MeV) and can keep narrow width even if the repulsive core becomes three times higher than that of the original potential. Even in the case of such strong repulsive core, the essence of our result remains unchanged.

D. Validity of our $\bar{K}N$ interaction

In this section, we comment on the $\bar{K}N$ interaction we use. When we discuss on the $\bar{K}N$ interaction, we should not confuse a bare one and an effective one (or $\bar{K}$-nucleus optical potential).

First, we consider the bare $\bar{K}N$ interaction. The Akaishi-Yamazaki $\bar{K}N$ interaction (AY $\bar{K}N$ interaction) employed in this paper is a bare $\bar{K}N$ interaction. We have already confirmed that the AY $\bar{K}N$ interaction has almost the same property as the chiral $\bar{K}N$ interactions for binding energies of $\bar{K}$ nuclear systems: the AY $\bar{K}N$ interaction gives −119 MeV attraction for a $\bar{K}$ in nuclear matter at the normal density, Weise's chiral $\bar{K}N$ interaction gives $-120\sim-130$ MeV attraction as seen in Fig. 3 of the first paper in Ref. [8] and the meson-exchange Jülich $\bar{K}N$ interaction gives $-103\sim-120$ MeV attraction in a similar treatment of in-medium propagation as shown in Fig. 2 of Ref. [14]. Thus, the AY $\bar{K}N$ interaction has the quite same property as other bare $\bar{K}N$ interaction as long as the binding energies of $\bar{K}$ nuclei are concerned. At the level of bare interaction, our empirically based $\bar{K}N$ interaction is very similar to those theoretically derived in other studies.

Next, we proceed to the effective interaction. The property of the effective interaction is strongly dependent on the prescription how to construct it from a bare interaction. The effective $\bar{K}N$ interaction led by our *g*-matrix method [1] is very attractive, whereas others [14–16] are less attractive. The latter employ Lutz's prescription [15], in which the optical potential of $\bar{K}$ for intermediate states is self-consistently treated. Here, we would like to present detailed comments about the difference of $\bar{K}$ optical potentials between cases of infinite nuclear matter and of few-body systems of our present concerns. In the former case the $\bar{K}$ is in a continuum level and its optical potential must reproduce "phase shift" of the $\bar{K}$-medium scattering state, whereas in the latter case the $\bar{K}$ is in a decaying bound state isolated far from continuum and its optical potential should reproduce not "phase shift" but "energy-level shift," because the phase shift no longer takes place due to the lack of incoming component in the decay-channel wave function. The *g* matrix in this situation has to be treated differently from the prescription given by Lutz and the other authors. The $\bar{K}$ self-mass should be introduced self-consistently not only in the intermediate-state spectrum but also in the starting energy of the *g*-matrix equation. This is a natural extension of the Brueckner-Bethe-Goldstone theory of nucleus where the self-consistency condition is imposed on both of the starting and intermediate-state energies. In our treatment, the imaginary parts of the propagator largely cancel out between the starting and the intermediate energies, and the resultant *g* matrix becomes closer to our *g* matrix used in the present AMD calculation.

We can directly confirm that $\bar{K}$ few-body systems should be treated by our prescription as follows. In Sec. IIIc of Ref. [1], it has already been demonstrated that our *g* matrix works well as an effective interaction for a $\bar{K}$ in few-body systems. Here, we refer to the result for a model $NNNK^-$ system interacting with a simple bare $\bar{K}N$ interaction of $v_{\bar{K}N}=-(500+i20)$ MeV $\exp[-(r/0.66\ \text{fm})^2]$ which keeps some

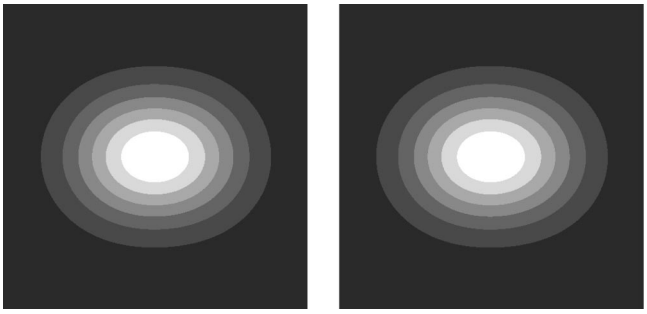

FIG. 1. Proton (left) and neutron (right) distributions of $|{}^{3}_{K}\mathrm{H}(T=0)\rangle$ obtained in the present calculation. The size of each frame is 3 fm$\times$3 fm.

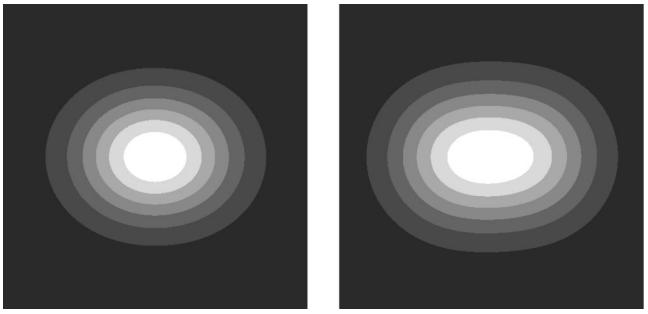

FIG. 2. Proton (left) and neutron (right) distributions of $ppnK^{-}$ which is an *intrinsic state in the isospin space* of $|{}^{3}_{K}\mathrm{H}(T=0)\rangle$.

essential property of the $\bar{K}N$ interaction used in the present paper. A variational calculation, which uses only the bare interaction, gives $E(\bar{K})=-107$ MeV and $\Gamma=24$ MeV. Our g matrix reproduces these values, namely, we obtained $E(\bar{K})=-109$ MeV and $\Gamma=29$ MeV which are in a good agreement with the variational result. On the other hand, if we use a g matrix obtained by the insertion of an optical potential, say $U^{\mathrm{opt}}=-(50+i100)$ MeV, to the intermediate-state energy spectrum in the propagation simulating "self-consistency" suggested in Refs. [14–16], we obtain $E(\bar{K})=-84$ MeV and $\Gamma=128$ MeV, which fails in reproducing the variational result. These facts give a justification of using our g matrix as an effective interaction in few-body calculations like AMD.

E. Interpretation of the density distribution

The influence of $pK^{-}/n\bar{K}^{0}$ mixing can clearly be seen in the density distribution. Figure 1 displays the density distribution of protons and neutrons in the $ppnK^{-}$ system calculated by the new framework. We can see that the proton distribution is almost the same as the neutron one, contrary to our previous result [3], where protons distribute more compactly than neutrons because of the strong attraction between the K^{-} and the proton. We can solve this contradiction by introducing the concept of an *intrinsic state in isospin space*, as follows: the calculated expectation value of $\boldsymbol{T}^{2}$ with the state $|\hat{P}_{T_z=0}\,\Phi\rangle$, in the case of $ppnK^{-}$, is nearly equal to zero. Therefore, this state is the eigenstate of isospin, i.e., $T=0$, and we express it as $|{}^{3}_{K}\mathrm{H}(T=0)\rangle$ hereafter. It is easily found that $|{}^{3}_{K}\mathrm{H}(T=0)\rangle$ is composed of two configurations concerning the z component of isospin:

$$\begin{aligned}\left|{}^{3}_{K}\mathrm{H}(T=0)\right\rangle &= \hat{P}_{T_z=0}[|\Phi_N\rangle\otimes|\varphi_K\rangle] \\ &= \hat{P}_{T_z=0}\left[\left(\sum_{m=-\infty}^{+\infty}\hat{P}_{T_z^N=m}\right)|\Phi_N\rangle \right. \\ &\quad \left. \otimes\left(\sum_{m=\pm 1/2}\hat{P}_{T_z^K=m}\right)|\varphi_K\rangle\right] \\ &= |\hat{P}_{T_z^N=1/2}\,\Phi_N\rangle\otimes|\hat{P}_{T_z^K=-1/2}\,\varphi_K\rangle \\ &\quad + |\hat{P}_{T_z^N=-1/2}\,\Phi_N\rangle\otimes|\hat{P}_{T_z^K=1/2}\,\varphi_K\rangle, \end{aligned} \tag{20}$$

where $\hat{P}_{T_z^N}$ and $\hat{P}_{T_z^K}$ are T_z projection operators for the nucleon system and the $\bar{K}$ meson, respectively. According to the values of T_z^N and T_z^K, the first term indicates $ppnK^{-}$, while the second term indicates $pnn\bar{K}^{0}$. Hereafter, we express them as $|ppnK^{-}\rangle$ and $|pnn\bar{K}^{0}\rangle$, respectively. In addition, the overlap between $|pnn\bar{K}^{0}\rangle$ and $e^{i\pi\hat{T}_y}|ppnK^{-}\rangle$, calculated numerically, is found to be almost one. Since this fact indicates $|pnn\bar{K}^{0}\rangle\simeq e^{i\pi\hat{T}_y}|ppnK^{-}\rangle$, we can say that our wave function satisfies

$$\left|{}^{3}_{K}\mathrm{H}(T=0)\right\rangle = \sum_{\theta=0,\pi} e^{i\,\theta\,\hat{T}_y}|ppnK^{-}\rangle = \sum_{\theta=0,\pi} e^{i\,\theta\,\hat{T}_y}|pnn\bar{K}^{0}\rangle. \tag{21}$$

Namely, the $|ppnK^{-}\rangle$ state rotates in isospin space so that $|{}^{3}_{K}\mathrm{H}(T=0)\rangle$, which has the good quantum number, $T=0$, is formed. Based on the analogy of an "intrinsic" state in a deformed nucleus, rotating in the space to form the eigenstate of the angular momentum, we can regard the $|ppnK^{-}\rangle$ or equivalent $|pnn\bar{K}^{0}\rangle$ as an *intrinsic state in the isospin space* of $|{}^{3}_{K}\mathrm{H}(T=0)\rangle$.

Figure 2 displays the proton and neutron distributions of the intrinsic state $|ppnK^{-}\rangle$. Clearly, the proton distribution is more compact than the neutron one; this fact is consistent with our previous study. Here, we note one point. Investigating the density distribution of $|pnn\bar{K}^{0}\rangle$, we find that its proton and neutron distributions are completely identical with the neutron and proton ones in the $|ppnK^{-}\rangle$, respectively. In other words, neutron distribution is more compact than proton one in the $|pnn\bar{K}^{0}\rangle$. After all, since Fig. 1 is drawn with the $|{}^{3}_{K}\mathrm{H}(T=0)\rangle$, which includes the $|ppnK^{-}\rangle$ and the $|pnn\bar{K}^{0}\rangle$ to form the eigenstate of isospin, the proton distribution is quite the same as the neutron one.

IV. RESULTS

Now that we have confirmed that the new framework works well, we proceed to an investigation of $pppK^{-}$,

TABLE IV. Summary of present calculations. J^π and T: spin parity and isospin of total system; $E(\bar{K})$: binding energy measured from the threshold of nucleus+$\bar{K}$; Γ: width decaying to $\Sigma\pi$ and $\Lambda\pi$ channels. $\rho(0)$: central density; $R_{\rm rms}$: root-mean-square radius of nucleon system; (β,γ): deformation parameters.

	J^π	T	E($\bar{K}$) (MeV)	Γ (MeV)	$\rho(0)$ (fm^{-3})	$R_{\rm rms}$ (fm)	β	γ (deg.)
$ppnK^-$	$\frac{1}{2}^+$	0	110.3	21.2	1.50	0.72	0.22	9.2
$pppK^-$	$\frac{1}{2}^-$	1	96.7	12.5	1.56	0.81	0.70	11.8
$pppnK^-$	1^-	$\frac{1}{2}$	105.0	25.9	1.29	0.97	0.54	3.8
^{6}BeK^-	0^+	$\frac{1}{2}$	104.2	33.3	0.91	1.17	0.44	0.3
^{9}BK^-	$\frac{1}{2}^-$	0	118.5	33.0	0.71	1.45	0.46	20.8
^{11}CK^-	$\frac{1}{2}^-$	0	117.5	46.0	0.81	1.48	0.35	46.5

$pppnK^-$, ^{6}BeK^-, ^{9}BK^-, and ^{11}CK^- with this framework. Since the intrinsic state of isospin space is found to be meaningful, as mentioned in the previous section, we generally denote $\bar{K}$ nuclei by their intrinsic states without any loss of validity; for example, ^3_KH is represented by $ppnK^-$. In all calculations, a single nucleon and $\bar{K}$ meson are described with two Gaussian wave packets and five, respectively, namely $N_n=2$ in Eq. (5) and $N_K=5$ in Eq. (7).

A. Binding energies

The results are summarized in Table IV. We determine J^π and T by assuming that nucleons occupy the configuration of the normal ground state and a $\bar{K}$ meson occupies the 0s state. Of course, as done in the prior section, we confirm after J and T projections that the expectation values of $\hat{\boldsymbol{J}}$ and $\hat{\boldsymbol{T}}$ are equal to those we set previously. Figure 3 displays the behavior of the total binding energy and the decay width, from $ppnK^-$ to ^{9}BK^-. The previous result [3] of ^{8}BeK^- is also shown. According to Table IV, all $\bar{K}$ nuclei are bound by about 100 MeV. Figure 3 shows us that the $\bar{K}$ nuclei except for $pppK^-$ are bound below the $\Sigma\pi$ threshold which is the main decay channel.

In Fig. 3 the thresholds of various decay modes are also shown, from which we can estimate the stability of $pppnK^-$ to ^{9}BK^- for the nucleon escaping process. First, $pppnK^-$ is found to be unstable for the nucleon escaping, since its total binding energy (112.5 MeV) is smaller than that of $ppnK^-+p$ (117.8 MeV). On the other hand, the deepest thresholds for ^{6}BeK^-, ^{8}BeK^-, and ^{9}BK^- are $ppnK^-+^3$He (125.3 MeV), $ppnK^-+\alpha+n$ (143.5 MeV) and ^{8}BeK^-+p(159.0 MeV), while their total binding energies are 131.7, 159.0, and 173.5 MeV, respectively. Therefore, ^{6}BeK^-, ^{8}BeK^-, and ^{9}BK^- are stable for the nucleon escaping. In the scope of the present study, ^{11}CK^- is also stable for the nucleon escaping because its total binding energy (190.9 MeV) is larger than that of ^{9}BK^-+deuteron (175.7 MeV).

As mentioned above, the K^- meson is bound by about 100 MeV in all of the $\bar{K}$ nuclei that we calculated. pK^- is bound by 27 MeV based on the initial assertion that it forms Λ (1405), and ppK^- is bound by 48 MeV according to [2]. Therefore, the binding energy of the K^- meson seems to be saturated in $\bar{K}$ nuclei heavier than $ppnK^-$. We think that this

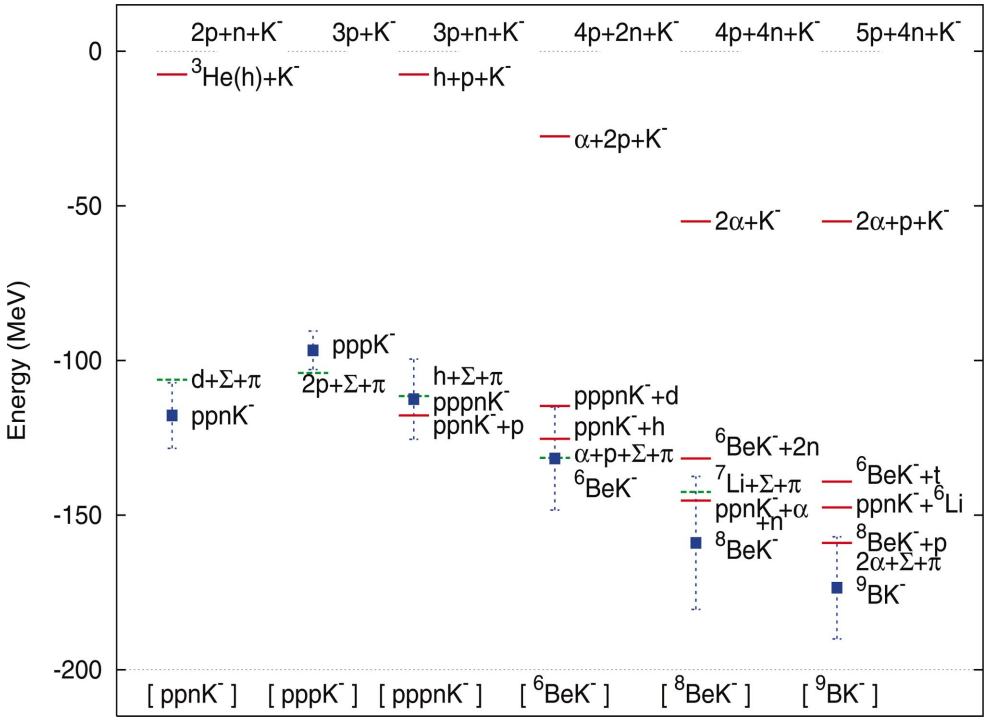

FIG. 3. (Color) Behavior of the total binding energy and the decay width, from $ppnK^-$ to ^{9}BK^-. The decay width is to $\Lambda\pi$ and $\Sigma\pi$ channels. The blue square and the vertical broken line indicates the binding energy and width of the $\bar{K}$ nucleus, respectively. The green-dashed line corresponds to the $\Sigma\pi$ threshold. The thresholds for other decay modes are expressed by the red lines.

TABLE V. $E(\bar{K})$ and number of strongly interacting nucleons near the $\bar{K}$ meson.

	$ppnK^-$	$pppK^-$	$pppnK^-$	^{6}BeK^-	^{9}BK^-	^{11}CK^-
$E(\bar{K})$	110.3	96.7	105.0	104.2	118.5	117.5
Nucleon	1.67	1.14	1.78	2.55	2.53	2.88

saturation of the binding energy is related to the range of the $\bar{K}N$ interaction. Since it is very short, the number of nucleons which a single K^- meson can interact with is limited. We count up the nucleons staying in the region where the $\bar{K}$ meson's density falls down from the maximum value $\rho^K_{\rm MAX}$ to $\frac{1}{5}\rho^K_{\rm MAX}$. In Table V, we show the number of strongly interacting nucleons ("Nucleon") staying around the $\bar{K}$ in various $\bar{K}$ nuclei. Except for $pppK^-$, which has a peculiar structure, as mentioned in a later section, about 1.7–2.9 nucleons are found to stay near the $\bar{K}$ meson.

B. Density distribution

Figure 4 displays the nucleon density distributions of $ppnK^-$, $pppK^-$, $pppnK^-$, ^{6}BeK^-, ^{9}BK^-, and ^{11}CK^-. It is found that $\bar{K}$ nuclei have extremely dense and peculiar nucleon distributions.

^{6}BeK^- has a two-center-like structure similar to ^{8}BeK^- [3]. Figure 5 shows proton and neutron distributions separately. We can find that protons have a two-center-like structure and that neutrons stay between two pairs of protons, against our expectation that ^{6}Be should have such a structure as $\alpha+2p$. We note that the $\bar{K}$ meson's density distribution, which is not displayed here, is very similar to the neutrons' one. The structure of ^{9}BK^- is quite similar to that of ^{8}BeK^- [3]. ^{11}CK^- has a three-cluster-like structure. Figure 6 shows the K^- meson distribution as well as the proton and neutron distributions in the intrinsic state of isospin space, namely pure ^{11}CK^- component. All clusters are attracted by a $\bar{K}$ meson being at the center of the system. Similarly to the case of $ppnK^-$, the proton distribution is more compact than the neutron distribution because the K^- meson attracts protons rather than neutrons.

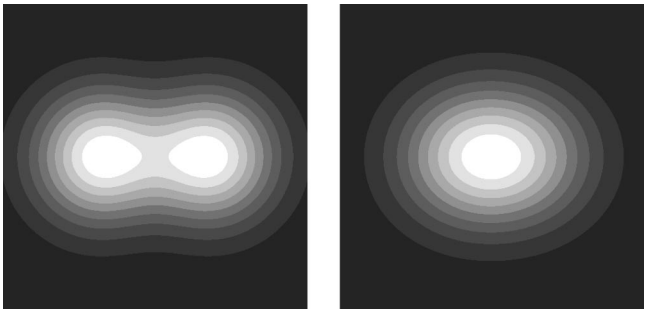

FIG. 5. Proton (left) and neutron (right) distributions of ^{6}BeK^-.

The most exotic system of $pppK^-$ shows a very peculiar density distribution. Strictly speaking, this system has not only the component of $pppK^-$, but also that of $ppn\bar{K}^0$ due to

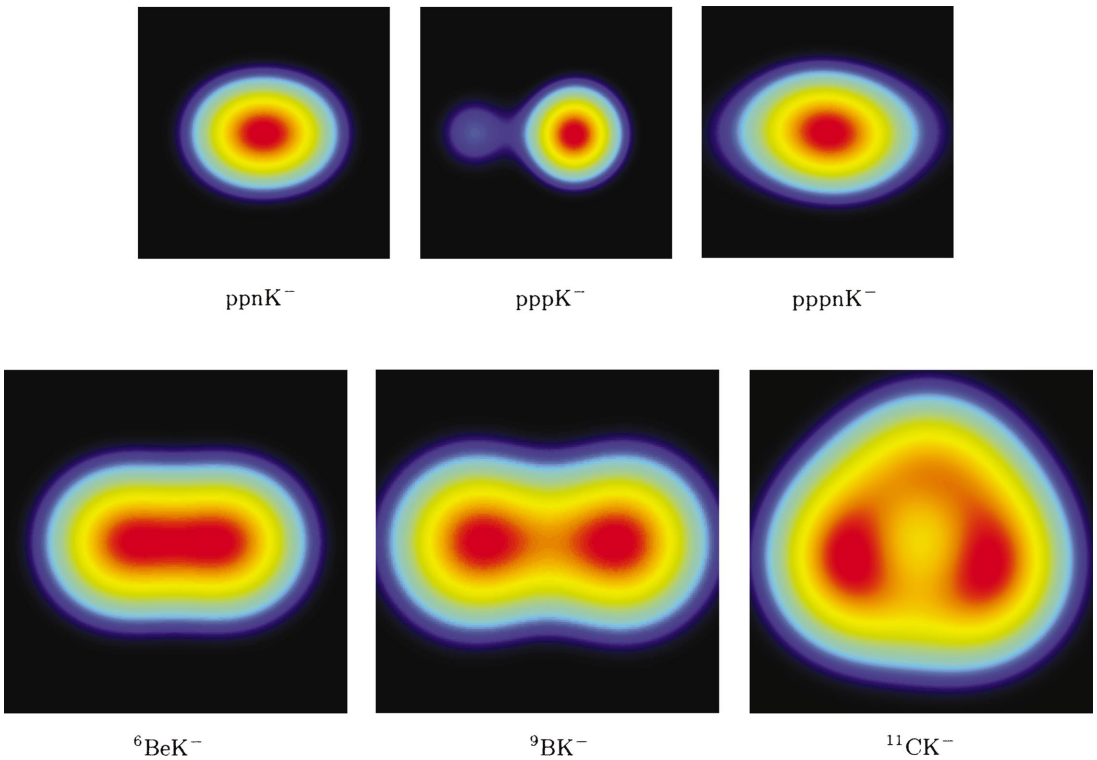

FIG. 4. (Color) Density contours of the nucleon distributions of various $\bar{K}$ nuclei. $ppnK^-$, $pppK^-$, and $pppnK^-$: 3 fm$\times$3 fm ^{6}BeK^-, ^{9}BK^-, and ^{11}CK^-: 4 fm$\times$4 fm.

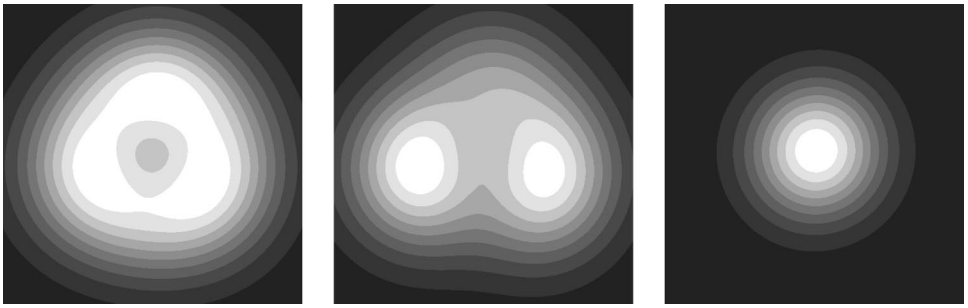

FIG. 6. Proton (left), neutron (middle), and K^- meson (right) distribtions of $^{11}CK^-$.

the $I=0$ $\bar{K}N$ interaction. We express this system as ${}^{3}_{K}$He. Figure 7 shows only proton density distribution extracted. We can see a "satellite" in this figure. Summing up the density of proton in the region of this satellite, we find that the proton number is nearly equal to one. Thus, this satellite is a single proton. In addition, the particle numbers of proton, neutron, K^- and $\bar{K}^0$ are 2.67, 0.33, 0.67, and 0.33, respectively. We can understand these particle numbers and the density distribution consistently as follows. We regard this system as a single proton combining ${}^{2}_{K}$H, following its density distribution (Fig. 7). In isospin space, ${}^{2}_{K}$H means the $|T=\frac{1}{2},T_z=\frac{1}{2}\rangle$ state, which is composed of two nucleons and a $\bar{K}$ meson. The weight of each component included is determined by Clebsch-Gordan coefficients as shown below:

$$
\begin{aligned}
|{}^{3}_{K}\mathrm{He}\rangle &= |p\rangle \otimes |{}^{2}_{K}\mathrm{H}\rangle = |p\rangle \otimes \left| T=\frac{1}{2},T_z=\frac{1}{2}\right\rangle \\
&= |p\rangle \otimes \left(\sqrt{\frac{2}{3}}\left| T^N=1,T_z^N=1;T^K=\frac{1}{2},T_z^K=-\frac{1}{2}\right\rangle \right. \\
&\quad \left. -\sqrt{\frac{1}{3}}\left| T^N=1,T_z^N=0;T^K=\frac{1}{2},T_z^K=\frac{1}{2}\right\rangle \right) \\
&= |p\rangle \otimes \left(\sqrt{\frac{2}{3}}|pp\otimes K^-\rangle + \sqrt{\frac{1}{3}}|pn\otimes \bar{K}^0\rangle \right). \qquad (22)
\end{aligned}
$$

The particle numbers counted according to Eq. (22) are the same as the above values. After all, we come to a conclusion that in ${}^{3}_{K}$He one proton keeps its identity and that the residual part is composed of ppK^- and $pn\bar{K}^0$, which are

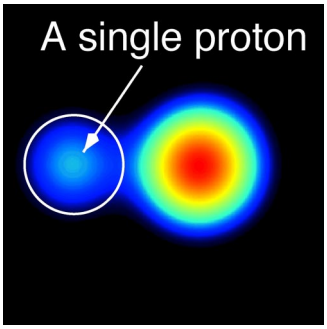

FIG. 7. (Color online) Proton distribution in $pppK^-$.

mixed due to the $I=0$ $\bar{K}N$ interaction. Note, however, that the single proton is strongly bound to ${}^{2}_{K}$H. In addition, we studied the dependence of this system on the number of wave packets. Even if one nucleon is represented by four Gaussian wave packets [i.e., $N_n=4$ in Eq. (5)], a proton is still pushed out, but a little less clearly. We consider that the third proton is pushed up to the 0*p*-shell due to Pauli blocking, so that it forms a satellite-like structure. $pppnK^-$ has an extra neutron compared to $pppK^-$. When a neutron is added to $pppK^-$, such a satellite-like structure disappears and a different structure is formed for $pppnK^-$.

C. Relativistic correction

The present calculations have been done in the nonrelativistic framework. The relativistic effect can be estimated by using a Klein-Gordon equation for $\bar{K}$,

$$
\left\{ -\frac{\hbar^2}{2m_K}\nabla^2 + U_{\mathrm{opt}} \right\} |\Phi\rangle = \left(\varepsilon_K + \frac{\varepsilon_K^2}{2m_K c^2} \right) |\Phi, \qquad (23)
$$

where ε_K is the energy of $\bar{K}$ without its rest mass. The optical potential, U_{opt}, is given as

$$
U_{\mathrm{opt}} = U_S + \frac{U_S^2}{2m_K c^2}, \qquad (24)
$$

on the assumption that the $\bar{K}$ is in a scalar mean field, U_S, provided by the shrunk nuclear core. When we make a mapping of energy;

$$
\left(\varepsilon_K + \frac{\varepsilon_K^2}{2m_K c^2} \right) \rightarrow \varepsilon_{\mathrm{map}}, \qquad (25)
$$

Eq. (23) becomes equivalent to a Schrödinger-type equation. We do with this equivalent equation. In this treatment, however, special cautions are necessary: the threshold energies of $\Lambda+\pi$ and $\Sigma+\pi$ and the complex energy of Λ (1405) also suffer the same mapping. The latter change requires refitting of the $\bar{K}N$ interaction parameters.

This scheme has been carried out in the case of $ppnK^-$. The binding energy and decay width are found to be $(B.E.,\Gamma_K)=(127,20)$ MeV. The binding energy increases by about 10% due to this relativistic effect.

V. SUMMARY

We improved the antisymmetrized molecular dynamics (AMD) regarding two points and applied it to systematic studies of $\bar{K}$ nuclei. One of our improvements is "$pK^-/n\bar{K}^0$ mixing," which enables us to treat directly the coupling of pK^- and $n\bar{K}^0$ through the $I=0$ $\bar{K}N$ interaction. The other one is " J and T projections" with which the strong isospin dependence of the $\bar{K}N$ interaction is expected to be correctly treated. Thus, AMD is capable of treating the $I=0$ $\bar{K}N$ interaction adequately, which plays an essential role in $\bar{K}$ nuclei.

We have investigated the properties of our new framework on $ppnK^-$. After J and T projections, the total system is found to possess the quantum numbers J and T, which turn out to be equal to those which we had assigned beforehand. Namely, we have confirmed that the J and T projections work correctly. The new result and the previous one are very similar to each other, but we can see the influence of $pK^-/n\bar{K}^0$ mixing in the density distributions of the protons and neutrons. Owing to the introduction of $\bar{K}^0$, the present wave function can form the eigenstate of isospin, i.e., $|{}^3_{\bar{K}}\mathrm{H}(T=0)\rangle$. When we draw the proton and neutron distributions of $|{}^3_{\bar{K}}\mathrm{H}(T=0)\rangle$, they are clearly different from those shown in our previous study. We confirm that the $|{}^3_{\bar{K}}\mathrm{H}(T=0)\rangle$ is formed by the rotation of $|ppnK^-\rangle$ in isospin space. Namely, $|ppnK^-\rangle$ is considered to be an "intrinsic state in isospin space" for the $|{}^3_{\bar{K}}\mathrm{H}(T=0)\rangle$. This intrinsic state $|ppnK^-\rangle$ is found to have quite the same proton and neutron distributions as those in our previous study. The $|{}^3_{\bar{K}}\mathrm{H}(T=0)\rangle$ contains both $|pnn\bar{K}^0\rangle$ and $|ppnK^-\rangle$ components with the same ratio. This is consistent with the fact that the calculated proton and neutron numbers are both equal to 1.5. The coupling of these two components due to the $I=0$ $\bar{K}N$ interaction helps the binding of the total system $|{}^3_{\bar{K}}\mathrm{H}(T=0)\rangle$.

We have studied $ppnK^-$, $pppK^-$, $pppnK^-$, ${}^6\mathrm{Be}K^-$, ${}^9\mathrm{B}K^-$, and ${}^{11}\mathrm{C}K^-$ with our new framework. All $\bar{K}$ nuclei that we investigated are bound by about 100 MeV below the threshold of each nucleus$+K^-$. Except for $pppK^-$, they are bound below the $\Sigma\pi$ threshold, which is the main decay channel. Since their decay width is 20–40 MeV and small compared to their binding energy, they appear to be discrete states. For the nucleon escaping process, $pppnK^-$ is found to be unstable, while ${}^6\mathrm{Be}K^-$, ${}^8\mathrm{Be}K^-$, and ${}^9\mathrm{B}K^-$ are stable. We found that they have very different structures. Especially, $pppK^-$ shows an interesting satellite-like structure which is composed of a single proton. This proton keeps its identity and is strongly bound by the main body.

According to our present study, we predict various deeply bound $\bar{K}$ nuclei. They have very peculiar structures with extremely high densities, which we have never seen. In the future, such $\bar{K}$ nuclei as those investigated in the present paper may be explored experimentally. For instance, $ppnK^-$ can be formed from a ${}^4\mathrm{He}$(stopped K^-,n) experiment [1,17]. An experiment at KEK has shown an indication for the predicted deeply bound state [19]. The use of inflight (K^-,N) reactions is also proposed [18]. Proton-rich exotic $\bar{K}$ nuclei are expected to be produced by (K^-,π^-) reactions via Λ^* doorway states [2]. In the present calculation, we assume that a bare $\bar{K}N$ interaction in the dense nuclear matter remains to be that in the free space. Our predictions will not only serve as guides for experimental search, but also provide benchmarks with which experimental binding energies will be compared. If deeper bound states are experimentally found, it would mean that modification of the bare $\bar{K}N$ interaction occurs in high density matter as a result of the restoration of chiral symmetry, as observed in the case of deeply bound pionic states [20], or that the hadronic phase is changed to a quark phase.

Finally, we would like to mention further possibility of the new framework of AMD. Since it can be extended straightforwardly to the case of multi $\bar{K}$'s, we can investigate multi-$\bar{K}$ nuclei, which are closely related to kaon condensation and strange quark matter [21,22]. The double-$\bar{K}$ nucleus, $ppnK^-K^-$, has been shown to be an even denser nucleus with a doubled binding energy [23]. The success of the new framework of AMD means that we can deal with even more fields of physics, because coupled-channel-like calculation can be carried out in the new version of AMD. For example, we can study Λ-Σ mixing in hypernuclei [24] with this new framework.

Note added in proof. Very recently, Suzuki *et al.* has discovered a neutral "strange tribaryon" [25]. This is interpreted as an isobaric analog state of the predicted $pppK^-$, whereas the observed K^- binding energy is significantly larger.

ACKNOWLEDGMENTS

One of the authors (A.D.) thanks Dr. M. Kimura for giving him graphic tools, and Dr. Y. Kanada-En'yo for fruitful discussions on our new framework. A.D. is financially supported by the JSPS. Part of the calculations in this paper are made using Scalar System Alpha1 in Yukawa Institute for Theoretical Physics. This work is supported by a Grant-in-Aid for Scientific Research of Monbukagakusho of Japan.

[1] Y. Akaishi and T. Yamazaki, Phys. Rev. C **65**, 044005 (2002).
[2] T. Yamazaki and Y. Akaishi, Phys. Lett. B **535**, 70 (2002).
[3] A. Doté, H. Horiuchi, Y. Akaishi, and T. Yamazaki, Phys. Lett. B **590**, 51 (2004).
[4] A. Doté, H. Horiuchi, Y. Akaishi, and T. Yamazaki, Prog. Theor. Phys. Suppl. **146**, 508 (2002).
[5] M. Iwasaki *et al.*, Phys. Rev. Lett. **78**, 3067 (1997); T. M. Ito *et al.*, Phys. Rev. C **58**, 2366 (1998).

[6] A. D. Martin, Nucl. Phys. **B179**, 33 (1981).
[7] A. Müller-Groeling, K. Holinde, and J. Speth, Nucl. Phys. **A513**, 557 (1990).
[8] T. Waas, N. Kaiser, and W. Weise, Phys. Lett. B **365**, 12 (1996); Phys. Lett. B **379**, 34 (1996); N. Kaiser, P. B. Siegel, and W. Weise, Nucl. Phys. **A594**, 325 (1995); W. Weise, *ibid.* **A610**, 35 (1996).
[9] Y. Kanada-En'yo, H. Horiuchi, and A. Ono, Phys. Rev. C **52**, 628 (1995); Y. Kanada-En'yo, H. Horiuchi, and A. Ono, Phys. Rev. C **52**, 647 (1995); Y. Kanada-En'yo, Phys. Rev. Lett. **81**, 5291 (1998).
[10] H. Kamada *et al.*, Phys. Rev. C **64**, 044001 (2001).
[11] A. Doté, Y. Kanada-En'yo, and H. Horiuchi, Phys. Rev. C **56**, 1844 (1997); A. Doté and H. Horiuchi, Prog. Theor. Phys. **103**, 91 (2000); **103**, 261 (2000).
[12] A. Ono, Ph.D. thesis.
[13] R. Tamagaki, Prog. Theor. Phys. **39**, 91 (1968).
[14] L. Tolos, A. Ramos, A. Polls, and T. T. S. Kuo, Nucl. Phys. **A690**, 547 (2001).
[15] M. Lutz, Phys. Lett. B **426**, 12 (1998).
[16] A. Ramos and E. Oset, Nucl. Phys. **A671**, 481 (2000); J. Schaffner-Bielich, V. Koch, and M. Effenberg, *ibid.* **A669**, 153 (2000); A. Cieply, E. Friedman, A. Gal, and J. Mares, *ibid.* **A696**, 173 (2001).
[17] M. Iwasaki, K. Itahashi, A. Miyajima, H. Outa, Y. Akaishi, and T. Yamazaki, Nucl. Instrum. Methods Phys. Res. A **473**, 286 (2001).
[18] T. Kishimoto, Phys. Rev. Lett. **83**, 4701 (1999).
[19] M. Iwasaki *et al.*, nucl-ex/0310018; M. Iwasaki *et al.*, Phys. Lett. B. (unpublished); T. Suzuki *et al.*, Proc. HYP2003 (unpublished).
[20] K. Suzuki *et al.*, Phys. Rev. Lett. **92**, 072302 (2004).
[21] D. B. Kaplan and A. E. Nelson, Phys. Lett. B **175**, 57 (1986).
[22] G. E. Brown, C. H. Lee, M. Rho, and V. Thorsson, Nucl. Phys. **A567**, 937 (1994); G. E. Brown, *ibid.* **A574**, 217c (1994); G. E. Brown and M. Rho, Phys. Rep. **269**, 333 (1996).
[23] T. Yamazaki, A. Doté, and Y. Akaishi, Phys. Lett. B **587**, 167 (2004).
[24] Y. Akaishi, T. Harada, S. Shinmura, and K. S. Myint, Phys. Rev. Lett. **84**, 3539 (2000); H. Nemura, Y. Akaishi, and Y. Suzuki, *ibid.* **89**, 142504 (2002).
[25] T. Suzuki *et al.*, Phys. Lett. B **597**, 263 (2004).